The study of the determination reasonable ⊏-type extinction grid based on the analysis of the electromagnetic field between the arcs, and the grid In the AC contacts machine

Yong Chol Jong[A] , Un Chol Ri [A*+], Gum Chol Ri[B], Chung Hyok Kim[A], Il Mo Ri[A] , Jong Chol Chu[A], Maek Zhang[A]

[A] *Faculty of renewable Energy Science, HamHung University of Hydraulics and Power, Ham Hung, D P R of Korea*
[B] *Faculty of Architecture Engineering, HamHung Construction University, Ham Hung, D P R of Korea*

*Correspondence: UnChol Ri, HamHung University of Hydraulics and Power, Ham Hung, D P R of Korea
[+] E-mail address: riunchol@163.com

ARTICLE INFO

Keywords:
extinction grid
arc

ABSTRACT

To improve the life of the appliance and ensure the full production capacity, it is important to improve the protection of the contactor.
In the literature, due to the inability to accurately determine the type of arc-extinguishing of contactors with multiple open points[1-4]. Therefore, the researchers did not determine a reasonable ⊏-type arc grid for enhancing the arc capacity.
This paper puts forward the problem of determining the electrodynamic force acting between the arc and the grid when the contact is open. The most reasonable ⊏-type arc grid is determined by the ANSYS application program, and the method of increasing the service life of the mechanism is introduced.

1. Study on the Electromechanical Forces Acting between the Arc and the grid in the ⊏-type arc grid

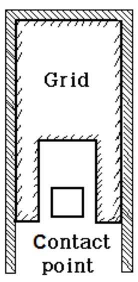

Fig1. ⊏-type extinction grid

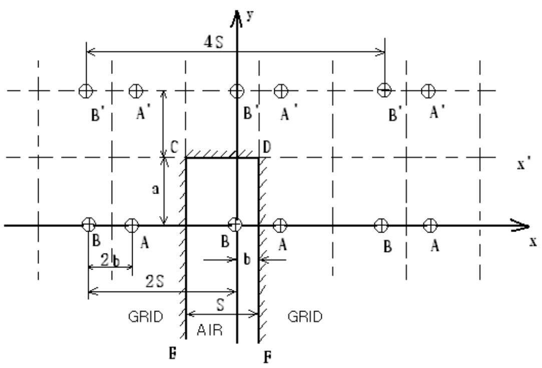

Fig2. Current system in the ⊏-type extinction grid

When the current signal I is at one point O of the c-shaped grating, the magnetic field between the conductor O and the steel grid can be used as a magnetic field in the current system as shown in Fig. 2.

In the absence of saturation in iron, these current sources have the same magnitude and direction as current I.

Surfaces FD and CE are both isostatic surfaces, and in some plans, the image projection formed by conductor O forms two sets of current systems, one set of A and the other set of B.

When conductor O is at the centerline of the recess, each image forms an electric current system case of b=s/2.

The magnetic field produced by each current path in the zone and the magnetic field produced by the conductor O in the recess is the same.

Thus, the interaction force between conductor O and its surrounding steel lattice can be converted to the sum of the forces acting between conductor O and its intermediate image.

For some conductors with a current value I, the flux functions they form at some point (x, y)in space when the distance between arcs is equal are.

$$\psi = -I \ln\left(ch\frac{2\pi}{l} y - \cos\frac{2\pi}{l} x \right) \qquad (1)$$

The strength of the magnetic field is

$$H_x = -\frac{\partial \psi}{\partial y},\ H_x = -\frac{\partial \psi}{\partial y},\ H_x = -\frac{\partial \psi}{\partial y}, \quad (2)$$

The force acting on the conductor O (x, y) is

$$\left.\begin{aligned} F_x &= -1.02\frac{2\pi}{l}I^2\left[\frac{\sin\frac{2\pi}{l}x}{ch\frac{2\pi}{l}y-\cos\frac{2\pi}{l}x}\right]10^{-7} \\ F_y &= -1.02\frac{2\pi}{l}I^2\left[\frac{sh\frac{2\pi}{l}x}{ch\frac{2\pi}{l}y-\cos\frac{2\pi}{l}x}\right]10^{-7} \end{aligned}\right\}, N$$

(3)

When choosing the sign of F_x, F_y, consider Bector's code rule and it is $F_x = +IH_y$, $F_y = -IH_x$.

The force acting on the arc in the ⊏-type grid using Equation 3 is shown in Fig. 2.

$$F_x = f_{Ax} + f_{Bx} + f'_{Ax} + f'_{Bx};$$

$$F_y = f_{Ay} + f_{By} + f'_{Ay} + f'_{By};$$

As shown in Figure 2, $f_{Ay}=0$, $f_{By}=0$ and $f'_{Bx}=0$, $f_{Bx}=0$ because B and B' are symmetric about point O.

Therefore

$$\left.\begin{aligned} F_x &= f_{Ax} + f'_{Ax} \\ F_y &= f'_{Ay} + f'_{By} \end{aligned}\right\} \quad (4)$$

at $A(x=-2b, y=0, l=2s)$

$$f_{Ax} = 1.02\frac{\pi}{s}I^2 ctg(\frac{\pi}{s}b)\cdot 10^{-7} \quad (5)$$

$A'(x=-2b, y=-2a)$

$$f'_{Ax} = 1.02\frac{\pi}{s}I^2\left[\frac{\sin\frac{2\pi}{s}b}{ch\frac{2\pi}{s}a-\cos\frac{2\pi}{s}b}\right]\cdot 10^{-7}$$

(6)

Substituting the repletion Coefficient σ and the Coefficient γ of the extinction of arc

$$F_x = 1.02\frac{\pi}{s}I^2\gamma\sigma\left[\frac{\sin\frac{2\pi}{s}b}{ch\frac{2\pi}{s}a-\cos\frac{2\pi}{s}b}+ctg(\frac{\pi}{s}b)\right]\cdot 10^{-7}$$

, (7)

also

$$F_y = 1.02\frac{\pi}{s}I^2\gamma\sigma\left[\frac{sh\frac{2\pi}{s}a}{ch\frac{2\pi}{s}a-\cos\frac{2\pi}{s}b}+cth(\frac{\pi}{s}b)\right]\cdot 10^{-7}$$

, (8)

Where $b = \frac{s}{2}$, we write Equation 7, 8 as following.

$$F_x = 1.02\frac{\pi}{s}I^2\gamma\sigma\left[\frac{\sin\frac{2\pi}{s}b}{ch\frac{2\pi}{s}a-\cos\frac{2\pi}{s}b}+ctg(\frac{\pi}{s}b)\right]\cdot 10^{-7} =$$

$$= 1.02\frac{\pi}{s}I^2\gamma\sigma\cdot ctg(\frac{\pi}{2})\cdot 10^{-7} = 0$$

$$F_y = 1.02\frac{\pi}{s}I^2\gamma\sigma\left[\frac{sh\frac{2\pi}{s}a}{ch\frac{2\pi}{s}a-\cos\frac{2\pi}{s}b}+cth(\frac{\pi}{2})\right]\cdot 10^{-7} =$$

$$= 1.02\frac{\pi}{s}I^2\gamma\sigma\left[\frac{sh\frac{2\pi}{s}a}{ch\frac{2\pi}{s}a-\cos\frac{2\pi}{s}b}+1.09\right]\cdot 10^{-7}$$

(9)

If s=2b, then $F_X=0$, so only the y-axis force is applied.

2. Reasonable ⊏-type extinction grid determination

Using Equation 9, I=320A to AC contact 6-40A and s=8~12mm, a=4~15mm, the Fy value is as below.

Table 1. Calculated value of Fy along a and s

a, mm / s, mm	4	5	6	7	8	9	10	11	12	13	14	15
8	4.114	4.205	4.248	4.268	4.277	4.281	4.283	4.284	4.284	4.284	4.284	4.285
9	3.597	3.700	3.750	3.781	3.794	3.800	3.805	3.806	3.807	3.808	3.808	3.808
10	3.182	3.291	3.354	3.388	3.406	3.416	3.422	3.424	3.426	3.427	3.427	3.427
11	2.840	2.954	3.020	3.062	3.086	3.099	3.106	3.110	3.030	3.114	3.115	3.116
12	2.560	2.670	2.743	2.788	2.815	2.830	2.842	2.847	2.851	2.853	2.854	2.855

Using the ANSYS application, the results obtained by changing the lattice groove dimensions with the above conditions under the condition of I = 320A are as follows.

Table 2. Calculated simulation value of Fy along a and s

a, mm / s, mm	4	5	6	7	8	9	10	11	12	13	14	15
8	4.112	4.216	4.270	4.274	4.271	4.275	4.288	4.285	4.289	4.302	4.311	4.319
9	3.582	3.612	3.654	3.712	3.745	3.784	3.792	3.797	3.801	3.803	3.803	3.803
10	3.193	3.268	3.359	3.381	3.395	3.397	3.411	3.417	3.420	3.423	3.423	3.424
11	2.891	3.011	3.014	3.072	3.095	3.164	3.179	3.188	3.199	3.167	3.112	3.154
12	2.546	2.643	2.697	2.735	2.789	2.812	2.820	2.821	2.825	2.835	2.845	2.877

Therefore, as shown in Tables 1 and 2, the value of F_y is the largest when a = 15mm and s = 8mm.

The dimensions of the ⊏-type extinction grid using the calculated value of the right are as follows.

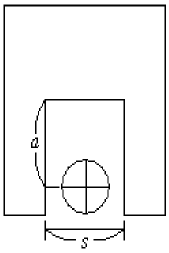

Figure 3. Reasonable ⊏-type extinction grid

Conclusion

Here, based on the precise consideration of the electromagnetic forces acting between the arc and the grid, the reasonable ⊏-type extinction grid are determined and the extinction of arc proceeds quickly, improving the lives of the apparatus.

Acknowledgements

The authors wish to thank Mr. RI who gave us much valuable helping in the early stages of this work.

AUTHOR CONTRIBUTIONS

Authors equally contributed.

ORCID

UnChol Ri http://orcid.org/0000-0002-4474-3389

References

[1] D. Pavelescu, G. Dumitrescu, S. Nitu et al. The influence of the axial magnetic field upon the low voltage electric arc in vacuum[J]. IEEE Transactions on Power Delivery, 1999, 14(3):948-953.

[2] Mercier, M, Cajal, D, Laurent, A, et al. Evolution of a low-voltage electric arc[J]. Journal of Physics D Applied Physics, 29(1):95-98.

[3] Debellut E, Cajal D, Gary F, et al. Phenomena generated by splitter plates on low-voltage electric arc dynamics[M]. 2004.

[4] L. Piqueras, D. Henry, D. Jeandel, et al. Three-dimensional modelling of electric-arc development in a low-voltage circuit-breaker[J]. 51(19-20):4973-4984.

[5] Pak A. Ya, Mamontov G. Ya. Boron Carbide Synthesis in Low-Voltage DC Electric Arc Initiated in Open Air[J]. Technical Physics Letters, 44(7):615-617.

[6] Brdys C, Toumazet J P, Laurent A, et al. Optical and magnetic diagnostics of the electric arc dynamics in a low voltage circuit breaker[J]. 2002, 13(13):1146.

[7] Mercier, M, Laurent, A, Velleaud, G, et al. Study of the movement of an electric breaking arc at a low voltage[J]. Journal of Physics D Applied Physics, 24(5):681-684.

[8] Hélène Rachard, Pierre Chévrier, Daniel Henry, et al. Numerical study of coupled electromagnetic and aerothermodynamic phenomena in a circuit breaker electric arc[J]. International Journal of Heat & Mass Transfer, 42(9):1723-1734.

[9] Ji, Liang, Chen, DeGui, Liu, YingYi, et al. Simulation of the interruption process of low voltage circuit breaker using dynamic mathematic arc model[J]. Proceedings of the Csee, 2009, 29(21):107-113.

[10] Na Lu, L. J. Xu, B. Miedziński. Approach for electrodynamic force for compensation in low voltage circuit breaker WP 630-1.2 type[J]. Journal of Zhejiang University-Science A(Applied Physics & Engineering), 2007, 8(3):393-396.

[11] Miedziński B. Approach for electrodynamic force for compensation in low voltage circuit breaker WP 630-1.2 type[J]. Journal of Zhejiang University(Science A:An International Applied Physics & Engineering Journal)(03):61-64.

[12] Trommler J, Koch S, Weiland T. Coupled simulation of switching arcs considering transient-capacitive effects[M]. 2014.

[13] 赵杰，李新福，潘立冬，等《 低压电器电弧投影温度场的重建》6(1) 7～9 . 低压电器，2006

[14] 胡辉，杨旗，包斌，何俊佳，李劲 《基于ANSYS 的空气电弧放电等离子体温度的数值模拟》 28（2）， 20～23. 电工电能新技术，2009

[15] 杨茜 等《低电断路器中空气电弧运动的仿真

机实验研究》26(15)　89～94.　中国电机工程学报，2006
[16]　Schade E,Shmelev D L　《Numerical simulation of high-current vacuum arcs with an external axial magnetic field》　31(5)　890～901.　IEEE Trane. Plasma Sci,　2003
[17] 陈德桂 等《交流接触器通断过程的只能操作》低压电器(1). 3-5. 2008.
[18 刘教民 等《开关电弧图像增强算法研究》中国电工技术学报(20) 20- 23. 2005.
[19] 王震洲 等《低压电器开关电弧图像增强的仿真图算法》电工技术学报(6). 50-54. 2008.
[20] 式延辉《一种适用于隔离开关的边缘提取法》35-127. 华中科技大学，2007.
[21] 李新福《低压电器电弧仿真研究》231-305. 河北工业大学，2004.
[22] 王震洲《低压电器开关电弧运动机理及仿真研究》251-296. 华北电力大学，2009.
[23] 王锟《 降低配网防雷间隙建弧率及电弧重燃率的方法研究》168-183.　广西大学，2008.